Immunity, Vol. 17, 809–822, December, 2002, Copyright ©2002 by Cell Press

Dynamics of p56lck Translocation to the T Cell Immunological Synapse following Agonist and Antagonist Stimulation

Lauren I. Richie Ehrlich,[1] Peter J.R. Ebert,[1] Matthew F. Krummel,[2,6] Arthur Weiss,[3] and Mark M. Davis[1,2,4,5]

[1]Program in Immunology
[2]Department of Microbiology and Immunology
Stanford University School of Medicine
Stanford, California 94305
[3]Department of Medicine and the
Howard Hughes Medical Institute
University of California, San Francisco
San Francisco, California 94143
[4]Howard Hughes Medical Institute
Stanford University School of Medicine
Stanford, California 94305

Summary

To study the spatio/temporal recruitment of lck during immunological synapse formation, we utilize high-speed time-lapse microscopy to visualize green fluorescent protein (GFP) fusions of lck and CD3ζ following agonist or altered peptide ligand (APL) stimulation. The dynamics of lck and CD3ζ recruitment are comparable; however, lck becomes excluded to the periphery of mature synapses, while most CD3ζ is centrally localized, suggesting a limited time frame within which lck can efficiently phosphorylate CD3 molecules during synapse maturation. Exposure of T cells to specific APLs affects the efficiency of conjugate formation and lck accumulation. Most surprisingly, we find an intracellular pool of lck associated with recycling endosomes that translocates to mature synapses within 10 min of calcium flux. This bolus of lck may contribute to intermediate-late signal transduction.

Introduction

T cell activation is initiated when T cell receptors (TCRs) bind stimulatory peptides in the context of self-major histocompatibility complex (MHC) molecules. This cell-surface recognition event initiates an intracellular signaling cascade that results in T cell activation and proliferation (Kane et al., 2000). One of the earliest intracellular modifications downstream of TCR recognition is p56lck (lck)-mediated tyrosine phosphorylation of CD3 ITAMs (Iwashima et al., 1994). While much is known about biochemical regulation of lck, little is known about its proximity to the TCR/CD3 during and after immunological synapse formation.

Lck has all of the prototypic domains of other src family kinases, rendering it capable of multiple protein-protein interactions (Wange and Samelson, 1996). Lck binds to the cytoplasmic tails of CD4 and CD8 via cysteine motifs in its unique N-terminal region (Turner et al., 1990). Engagement of CD4 along with CD3 has been shown to enhance T cell responses in an lck-dependent manner (Abraham et al., 1991; Anderson et al., 1987; Glaichenhaus et al., 1991). This augmented activation is thought to be due to lck autophosphorylation on tyrosine 394. However, it has not been clearly demonstrated that physiological antigens mediate lck autophosphorylation (Luo and Sefton, 1990). Nonetheless, lck, CD4, and CD3 can form a trimolecular complex (Rudd et al., 1991), bringing lck into proximity with CD3 ITAMs to initiate tyrosine phosphorylation.

Lck SH3 and SH2 domains are also important regulators of kinase activity. Lck can be activated via SH3 domain-mediated interactions with the costimulatory molecule CD28 (Holdorf et al., 1999). The lck SH2 domain can interact with the tyrosine kinase ZAP-70 and with CD3ζ ITAMs. Deletion of or mutation within this domain reduces CD3ζ and ZAP-70 association and phosphorylation and greatly impairs T cell activation (Lewis et al., 1997; Straus et al., 1996). Furthermore, lck can be activated by interactions with the tyrosine phosphatase CD45 (Trowbridge and Thomas, 1994).

These protein-protein interactions regulate lck's activity and proximity to effectors, making lck a likely candidate for spatial regulation during T cell activation. A number of studies have recently described the spatial and temporal recruitment of lck-interacting proteins at the immunological synapse. By immunological synapse, we mean a stable contact region between T cells and APCs that displays a broad, flat interface. Seminal work by the laboratories of Kupfer and Dustin on T cell:APC conjugates demonstrated that adhesion molecules such as LFA-1 were recruited to the synapse periphery, termed the p-SMAC (peripheral supramolecular activation cluster), while signaling molecules such as TCR/CD3 and PKC-θ were concentrated in the central region of the synapse, the c (central)-SMAC (Dustin et al., 1998; Monks et al., 1998). Confirmation of this spatial organization during a productive T cell interaction has come from real time studies of labeled APC molecules in artificial membranes (Grakoui et al., 1999) and GFP-labeled surface molecules in T and B cells (Krummel et al., 2000).

Previously, in retrospective mature T cell conjugates, we made the preliminary observation that lck was localized to the periphery of the mature T cell synapse, while CD3ζ was in the center (Richie et al., 2002). Given the complex distribution of lck-interacting proteins at the immunological synapse, we wished to extend these observations to precisely define the temporal and spatial recruitment of lck during mature immunological synapse formation. To this end, we expressed an lck-GFP fusion protein in two different T cell systems and imaged conjugate formation in real time. We find that lck is rapidly recruited to the immunological synapse following agonist stimulation. Within 15 s of calcium flux, lck accumulates at the synapse periphery, but in the next few minutes lck moves dynamically within the synapse, eventually settling into a peripheral accumulation pattern, colocalizing with CD4. These data suggest a limited time for maximal lck interaction with CD3 at the onset of synapse

[5]Correspondence: mdavis@cmgm.stanford.edu
[6]Present address: Department of Pathology, University of California San Francisco, San Francisco, California 94143.

formation. We also examined the recruitment of lck to the synapse following altered peptide ligand (APL) stimulation. We find that the temporal and spatial patterns of lck recruitment do not differ between strong and weak agonists, but the efficiency of conjugate formation is reduced in the later case. Furthermore, antagonists do not induce efficient conjugate formation. We also describe an intracellular pool of lck in both T cell systems, confirming the previous observations of Ley et al. (1994) in Jurkat T cells. We find that this pool surrounds the microtubule organizing center (MTOC), colocalizes with recycling endosomes, and translocates to the interface following agonist but not antagonist stimulation.

Results

Lck-GFP Is Functional and Does Not Interfere with T Cell Receptor-Mediated Activation

As previously reported, we made a carboxy-terminal lck-GFP fusion with a four amino acid linker, PVAT (Richie et al., 2002). To ensure that lck-GFP was functional, it was expressed in JCAM1.6 cells, a Jurkat mutant lacking lck activity and unable to flux calcium following TCR stimulation (Straus and Weiss, 1992). Both wild-type lck and the lck-GFP fusion are able to restore calcium flux in JCAM1.6 cells following TCR ligation (Supplemental Figure S1A at http://www.immunity.com/cgi/content/full/17/6/809/DC1). The identity of the GFP-fusion was confirmed by Western blot (data not shown). Therefore, our lck-GFP fusion is functional and can be activated by TCR ligation.

We also ascertained whether expression of lck-GFP altered T cell proliferative capacity. Lck-GFP was subcloned into a retroviral vector, and the D10 T cell line was stably transduced. The D10 TCR is activated by a peptide of conalbumin (CA134-146) in the context of I-A^k (Kaye et al., 1983). A comparison of wild-type and transduced D10 T cells shows that lck-GFP does not alter D10 proliferation over a range of conalbumin concentrations (Supplemental Figure S1B at http://www.immunity.com/cgi/content/full/17/6/809/DC1). Therefore, we proceeded to examine the spatial and temporal localization of lck-GFP at the immunological synapse.

Lck-GFP Translocates to the Immunological Synapse following Agonist but Not Antagonist Stimulation in D10 T Cells

To observe lck translocation to the immunological synapse, lck-GFP D10 cells were imaged as they interacted with CA-pulsed CH27 B cells. The T cells were loaded with the calcium indicator dye fura-2 before imaging. Agonist-pulsed CH27 B cells were added to the T cells, and images were acquired for 15 min at 15 s time intervals. At each interval, four images were acquired: first, a differential interference contrast (DIC) image, second and third 340 nm and 380 nm images for calcium analysis, and fourth a 20 μm z stack of GFP images acquired at 1 μm intervals. From this z stack, we generated 3-dimensional (3-D) reconstructions of lck-GFP that were rotated to view the immunological synapse en face. In addition, we followed a central horizontal GFP slice of the cell over time.

As seen in Figure 1A, when the front edge of a crawling D10 cell contacts an agonist-pulsed CH27 B cell, it forms a flat interface, rapidly fluxes calcium, and accumulates membrane localized lck-GFP at the interface (see Supplemental Movie S1 at http://www.immunity.com/cgi/content/full/17/6/809/DC1 for the full timecourse). Interestingly, a large intracellular pool of lck-GFP is present in D10 cells, and it translocates toward the interface, frequently resulting in a trail of lck-GFP between the intracellular pool and the membrane accumulation (Figure 1A, last two frames). Within the synapse, lck-GFP moves rapidly from the periphery to a more central region within the first couple of minutes post calcium flux (compare the 1 min to the 2 min time point). Then lck-GFP moves to the periphery of the synapse until the intracellular pool translocates to the interface, obscuring the precise membrane lck localizations (compare 4 and 5 min time points to the 7 min time point).

We also examined lck-GFP accumulations at the immunological synapse following stimulation with the antagonist E8T (Dittel et al., 1997). When a D10 cell contacts an E8T-pulsed CH27 B cell, a tight interface can form between the cells. However, calcium flux is transient, and lck-GFP does not accumulate at the contacting membranes. Furthermore, the intracellular lck pool does not translocate to the interface (Figure 1B and Supplemental Movie S2 at http://www.immunity.com/cgi/content/full/17/6/809/DC1 for the complete timecourse). In retrospective agonist conjugates imaged 30 min after T cell:B cell admixture, the intracellular pool is no longer a distinct entity, as it accumulates at the contacting interface (Supplemental Figure 2A and Supplemental Movie S3 at http://www.immunity.com/cgi/content/full/17/6/809/DC1). In contrast, retrospective E8T conjugates continue to display a distinct intracellular pool (Supplemental Figure 2B and Supplemental Movie S4 at http://www.immunity.com/cgi/content/full/17/6/809/DC1). Specifically, 86% of CA retrospective conjugates display translocation of the intracellular lck pool, in contrast to 35% of E8T conjugates.

To quantitate the relative amount of lck-GFP at the immunological synapse following agonist and antagonist stimulation, the average intensity at the T cell:B cell interface was compared to the rest of the cell membrane during conjugate formation. Following CA stimulation, lck-GFP accumulates to a 1.5-fold level at the interface within 3 min of calcium flux, and this level is maintained for at least 13 min. In contrast, there is no significant accumulation of lck-GFP at the interface following stimulation with the antagonist E8T (Figure 3A).

To further characterize the difference between agonist and antagonist stimulation, the efficiency of conjugate formation was compared. On a given day, random fields of D10 cells interacting with either CA-pulsed or E8T-pulsed CH27 cells were scored for the number of T cell:B cell front contacts and the number of conjugates. Cells were scored positive for conjugation if they stopped migrating, formed a flat interface with a B cell, and fluxed calcium. As seen in Figure 3D, the efficiency of conjugate formation is 80% with the agonist peptide CA, but only with 10.3% with the antagonist E8T. In summary, CA induces more efficient conjugate formation, lck-GFP accumulation, and translocation of the intracellular lck pool.

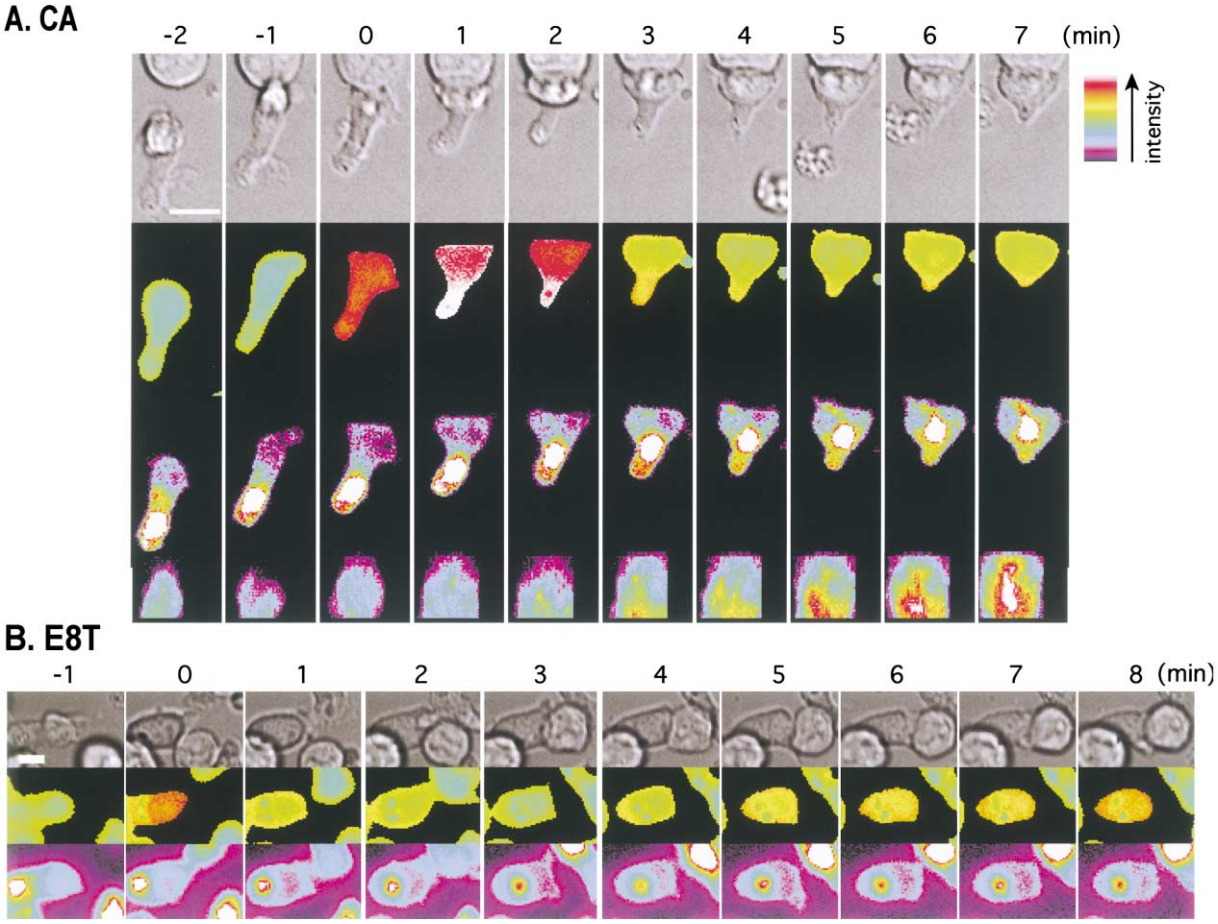

Figure 1. lck-GFP Is Rapidly Recruited to the D10 T Cell Immunological Synapse following Agonist but Not Antagonist Stimulation

Fura-2 loaded lck-GFP D10 T cells were imaged as they interacted with agonist CA (A)- or antagonist E8T (B)-pulsed CH27 cells. Time-lapse images were taken every 15 s for 15 min. The top row consists of DIC images; the second row contains fura-2 excitation ratios; the third row contains GFP images of single horizontal slices through the center of the cell; the fourth row (A) contains a 3-D reconstruction of lck-GFP at the immunological synapse viewed en face. Time 0 corresponds to the initial rise in intracellular calcium. Scale bars, 10 μm. See Supplemental Movies S1 and S2 at http://www.immunity.com/cgi/content/full/17/6/809/DC1 for complete timecourses of (A) and (B), respectively.

Lck-GFP Accumulates Efficiently at the Interface to Agonist and Weak Agonist but Not Antagonist Stimulation in 5C.C7 T Cell Blasts

To confirm our results in the D10 T cell line, we utilized a second T cell system, 5C.C7 TCR transgenics. We transduced freshly activated 5C.C7 T cell blasts with lck-GFP and imaged conjugate formation with peptide-pulsed CH27 cells several days later. The 5C.C7 TCR is activated by a peptide of moth cytochrome C (MCC 88-103) in the context of I-E^k (Fazekas de St. Groth et al., 1993). 102S is a well-characterized weak agonist peptide while 99R is an antagonist (Rabinowitz et al., 1996b).

As seen in Figure 2A, when a 5C.C7 blast contacts a MCC-pulsed CH27 B cell, it rapidly fluxes calcium and forms a tight interface. Membrane localized lck-GFP quickly translocates to the immunological synapse (see Supplemental Movie S5 at http://www.immunity.com/cgi/content/full/17/6/809/DC1 for the complete timecourse). The 3-D reconstructions demonstrate that lck-GFP accumulates centrally shortly following calcium flux (see the 0 min time point), though the very first strong accumulation is peripheral (see the first frame of calcium flux in Supplemental Movie S5 at http://www.immunity.com/cgi/content/full/17/6/809/DC1). Within a few minutes, lck accumulates preferentially in the p-SMAC (compare 1:30 min time point to 2:15 and subsequent time points). Unlike D10 cells, 5C.C7 blasts do not display a bright intracellular pool of lck-GFP. However, upon closer examination, such a pool can be seen, as at the 2:15 and the 4:30 time points just behind the interface. Furthermore, intracellular lck can be seen prior to conjugate formation at the rear of the cell in Supplemental Movie S5 (http://www.immunity.com/cgi/content/full/17/6/809/DC1), indicating that it is not a result of activation-induced endocytosis. Interestingly, this pool often corresponds to a region of less intensity in the fura-2 signal, suggesting colocalization with endosomes (compare the fura-2 images to the GFP images at 2:15 and 4:30 in Figure 2A).

As lck associates with CD4, we wished to test whether CD4 capping was sufficient to induce lck recruitment. We observed that antibodies to CD4 but not to CD3

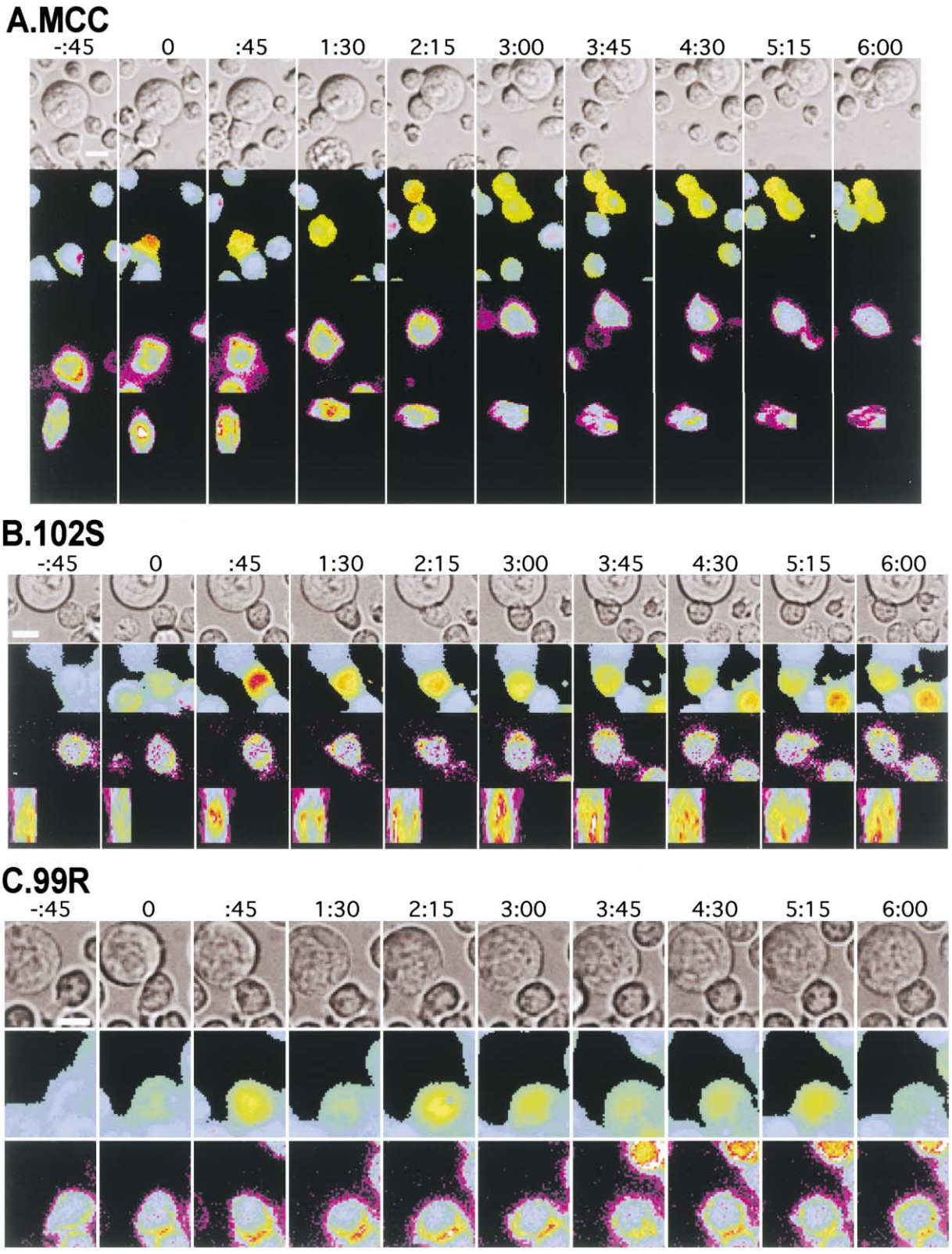

Figure 2. lck-GFP Translocates to the Immunological Synapse in 5C.C7 T Cell Blasts following Agonist and Weak Agonist but Not Antagonist Stimulation

Fura-2 loaded Lck-GFP 5C.C7 T cell blasts were imaged as they interacted with agonist MCC (A)-, weak agonist 102S (B)-, or antagonist 99R (C)-pulsed CH27 B cells. The rows are arranged as for Figure 1A. Time is displayed above each panel as min:sec elapsed after the onset of calcium flux, which is set as time 0. Color scale as for Figure 1. Scalebar, 10 μm. See Supplemental Movies S5, S6, and S7 at http://www.immunity.com/cgi/content/full/17/6/809/DC1 for complete timecourses of (A), (B), and (C), respectively.

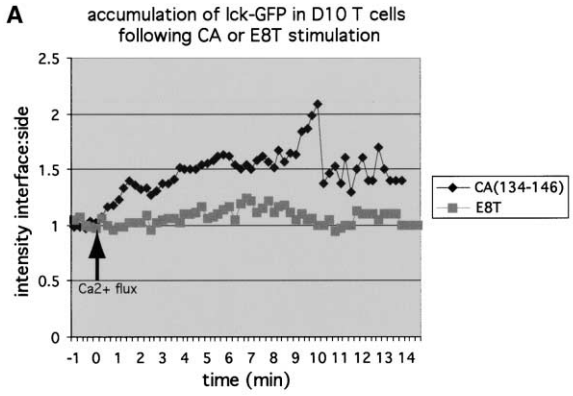

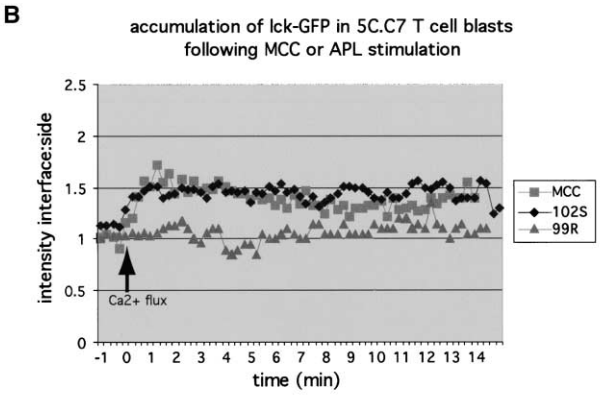

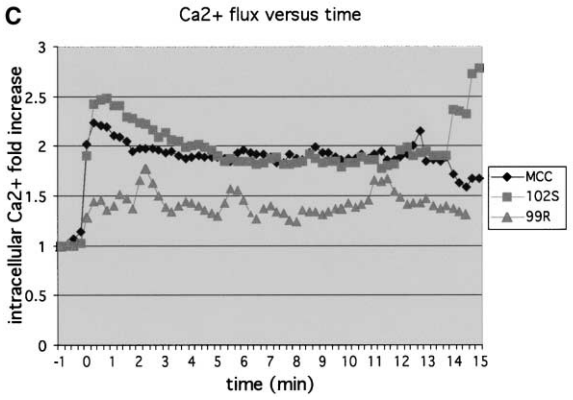

D

Cell type	Peptide	# front contacts	#contacts	#conjugates	Efficiency
D10	CA	40		32	80%
D10	E8T	58		6	10.3%
5C.C7	MCC		176	115	65.3%
5C.C7	102S		152	62	40.7%
5C.C7	99R		176	12	6.8%

Figure 3. Quantitation of lck Accumulations, Calcium Flux, and Efficiency of Conjugate Formation following Agonist and APL Stimulation

(A) During conjugate formation, lck-GFP D10 cells were scored for the average GFP intensity at the interface/average intensity on the remaining cell membrane. Regions at the interface or the noncontacting portion of the cell were traced in Metamorph (Universal Imaging), and after subtraction of background fluorescence from an adjacent empty region, the ratio of the average intensity of the two regions was calculated. The mean of ratios from different conjugates was calculated and displayed versus time. n = 20 agonist and 9 antagonist conjugates.

(B) 5C.C7 conjugates were scored for lck-GFP accumulations as in (A). n = 19 agonist, 14 weak agonist, and 3 antagonist conjugates.

(C) lck-GFP 5C.C7 blasts were scored for fold increase of intracellular calcium following activation. n = 10 agonist, 10 weak agonist, and 4 antagonist conjugates. Time 0 is defined as the onset of calcium flux in all graphs.

(D) Random fields of D10 cells or 5C.C7 cells on the same day were observed for conjugate formation with peptide pulsed CH27 cells. Front contacts were scored for D10 cells when the leading edge of the cell contacted an APC. 5C.C7 cells were scored for the total number of B cell contacts since the front edge could not be easily distinguished. The efficiency of conjugate formation was determined as the # conjugates/# (front) contacts × 100.

were able to co-cap lck-GFP, indicating that synapse localized lck is CD4-associated (see Supplemental Figure S3 at http://www.immunity.com/cgi/content/full/17/6/809/DC1). Furthermore, lck-GFP was not co-capped with CD28 (see Supplemental Figure S3 at http://www.immunity.com/cgi/content/full/17/6/809/DC1).

To determine whether lck recruitment is affected by APL stimulation, we examined translocation of lck-GFP in response to the weak and strong agonists. In Figure 2B, the weak agonist 102S induces calcium flux and rapid lck-GFP accumulation at the interface. Lck-GFP first accumulates in a central region (see 45 min time point), then at the synapse periphery over the next several minutes (compare:45 to 1:30 and subsequent time points. See Supplemental Movie S6 at http://www.immunity.com/cgi/content/full/17/6/809/DC1 for the complete timecourse). Thus, strong and weak agonists induce similar temporal and spatial recruitment of lck-GFP. In contrast, the antagonist 99R does not induce lck-GFP translocation even when calcium elevation and a flat interface are observed (Figure 2C and Supplemental Movie S7 at http://www.immunity.com/cgi/content/full/17/6/809/DC1). Furthermore, translocation of the intracellular lck-GFP pool can be observed in blasts following 102S stimulation (compare fura-2 and GFP images between :45 and 3 min time points in Figure 2B), but not 99R stimulation (see 3:45-5:15 time points in Figure 2C).

To quantitate lck-GFP accumulations during agonist and APL stimulation, the average intensity of GFP at contacting interfaces was compared to the rest of the cell membrane. Figure 3B shows that within 1 min of calcium flux, lck-GFP accumulates to a 1.5-fold level at the immunological synapse following MCC and 102S

stimulation. In contrast, there is no accumulation seen for the antagonist 99R.

Two additional criteria were considered for distinguishing between agonist and weak agonist stimulation. First, the magnitude and duration of calcium flux were measured. As seen in Figure 3C, both MCC and 102S stimulation induce a rapid rise in calcium that plateaus at 2-fold over background. In contrast, 99R induces a smaller calcium flux that is transient and periodic. As the graph represents an average, it does not reflect that calcium levels return to baseline and spike periodically following antagonist stimulation in individual cells (data not shown). The second criterion considered was the efficiency of conjugate formation. In random fields, 5C.C7 blasts were scored for total contacts made and the number of conjugates formed with CH27 B cells. As seen in Figure 3D, the efficiency of 5C.C7 blast conjugate formation is 65.3% to MCC, 40.7% to 102S, and 6.8% to 99R stimulation. In summary, while neither the spatial or temporal accumulations of lck-GFP nor the magnitude or duration of calcium flux distinguish between strong and weak agonist stimulation, conjugate formation is more efficient with the strong agonist MCC. The antagonist 99R fails to induce lck-GFP accumulation, generates a smaller and less sustained calcium flux, and reduces the efficiency of conjugate formation.

CD3ζ-GFP Accumulates with Similar Dynamics but Different Spatial Localization within the Immunological Synapse

We examined the spatial and temporal recruitment of CD3ζ in the 5C.C7 system for direct comparison to lck. 5C.C7 T cell blasts were transduced with CD3ζ-GFP (Richie et al., 2002) and were imaged several days later during conjugate formation. As seen in Figure 4A, CD3ζ is rapidly recruited to the immunological synapse following calcium flux (compare 1:30 to 1:30, and see Supplemental Movie S8 at http://www.immunity.com/cgi/content/full/17/6/809/DC1 for the complete timecourse). At time point 0, the first accumulations of CD3ζ are at the periphery of the synapse, but over time, CD3ζ is recruited into one predominant accumulation at the center of the synapse (compare time point 0 to time points 3 and 12). This is consistent with the pattern and kinetics of CD3ζ accumulation as reported previously in D10 cells (Krummel et al., 2000).

To compare CD3ζ and lck, we quantified the fold increase of CD3ζ-GFP intensity at the interface during conjugate formation. As seen in Figure 4B, both molecules are recruited to the synapse with remarkably similar kinetics. One minute after calcium flux, they accumulate at slightly more than a 1.5-fold level, and this accumulation is maintained for at least 13 min post calcium flux. Therefore, lck and CD3ζ are temporally coordinated at the synapse. We next compared the spatial accumulations of lck and CD3ζ in more detail.

Lck-GFP and CD3ζ-GFP 5C.C7 blasts were allowed to interact with MCC-pulsed CH27 B cells at least 30 min before imaging. We then generated 3-D reconstructions, which were rotated to view the immunological synapse en face. As seen in Figure 5A and B, lck-GFP is predominantly found in peripheral accumulations, while CD3ζ-GFP is found in central accumulations. Specifically, 68% of retrospective conjugates display a central CD3ζ accumulation while 70% demonstrate peripheral lck accumulations (Figure 5C). These data suggest that lck is recruited to the periphery of mature synapses providing a limited time in which it can interact efficiently with CD3 ITAMS.

To address the temporal window of lck and CD3ζ interactions more directly, the synapse accumulation patterns of both molecules were compared throughout the duration of conjugate formation. To this end, four synapse patterns were scored as previously described (Richie et al., 2002). In brief, interfaces were defined by the flat region at the T cell:CH27 junction. Accumulations that extended to the periphery of the interface but were absent from the center were scored as excluded; central accumulations were those in the middle of the interface that did not extend to the periphery; uniform accumulations were evenly distributed across the interface; and excluded + central patterns displayed discreet central and peripheral accumulations. Figure 5D quantitates the percentage of conjugates displaying the four accumulation patterns over time. Immediately following calcium flux, both lck and CD3ζ are predominantly at the periphery of the synapse. Within the next few minutes both molecules display uniform and excluded + central accumulations. During these first few minutes, lck has an opportunity to interact with and phosphorylate CD3ζ ITAMs. Over the next 10–15 min, an increasing percentage of conjugates display peripheral lck accumulations and central CD3ζ accumulations, indicating that the molecules become spatially separated. However, it should be noted that both lck and CD3ζ move dynamically throughout the interface at all time points. Thus, while CD3ζ and lck are predominantly localized centrally and peripherally, respectively, at later time points, conjugates that deviate from this pattern are found at lower frequencies (Figure 5D). Such a central accumulation of lck during a period in which lck is predominantly excluded can be seen at the 4:30 time point in Figure 2A.

To confirm that endogenous lck and TCR display similar accumulation patterns, we performed immunofluorescence on retrospective 5C.C7-CH27 conjugates. As seen in Figure 6, lck and CD4 largely colocalize at the immunological synapse periphery, while Vβ3 is found in the center, consistent with patterns observed using GFP fusions. However, it should be noted that this spatial resolution does not allow us to distinguish between molecules at the cellular membrane and those within vesicles just below the surface. Therefore, it is possible that Vβ3 has been internalized. The peripheral CD4 accumulation in 5C.C7 cells is consistent with previous observations in D10 cells (Krummel et al., 2000). To establish a direct comparison between CD4 and the prototypical peripheral synapse marker LFA-1, we performed immunofluorescent analysis on these two proteins. As seen in Figure 6, both CD4 and LFA-1 colocalize to the synapse periphery, confirming that CD4 is a peripheral marker.

An Intracellular Pool of lck Surrounds the MTOC and Is Colocalized with Recycling Endosomes

Though an intracellular pool of lck has been previously described in Jurkat T cells (Ley et al., 1994), we wanted to ensure that this pool was not a result of mislocalization of the GFP fusion protein. Therefore, we stained endogenous lck in both D10 and 5C.C7 T cells. The

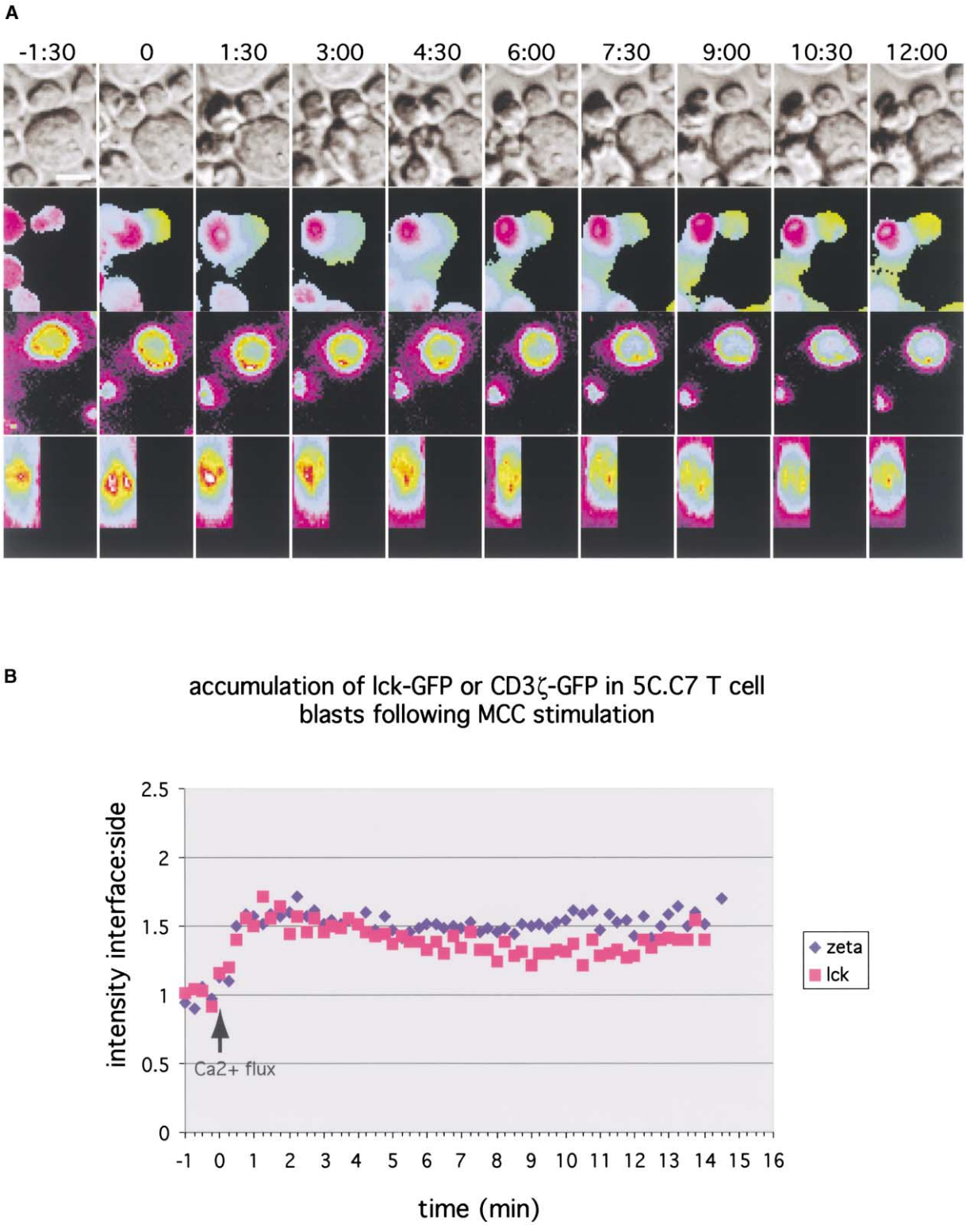

Figure 4. Accumulation of CD3ζ-GFP at the Immunological Synapse Is Temporally Similar but Spatially Distinct from lck-GFP

(A) Fura-2 loaded CD3ζ-GFP 5C.C7 blasts were imaged as they interacted with MCC-pulsed CH27 B cells. The images, color scale, and time are arranged as for Figure 1. See Supplemental Movie S8 at http://www.immunity.com/cgi/content/full/17/6/809/DC1 for the complete timecourse. Size bar, 10 μm.

(B) To quantitate the accumulation of CD3ζ-GFP at the synapse over time, the relative GFP intensity of 18 conjugates at contact membranes versus noncontacting membranes was scored and averaged as in Figure 3. The graph was then overlayed with the comparable lck-GFP graph to allow for direct comparison.

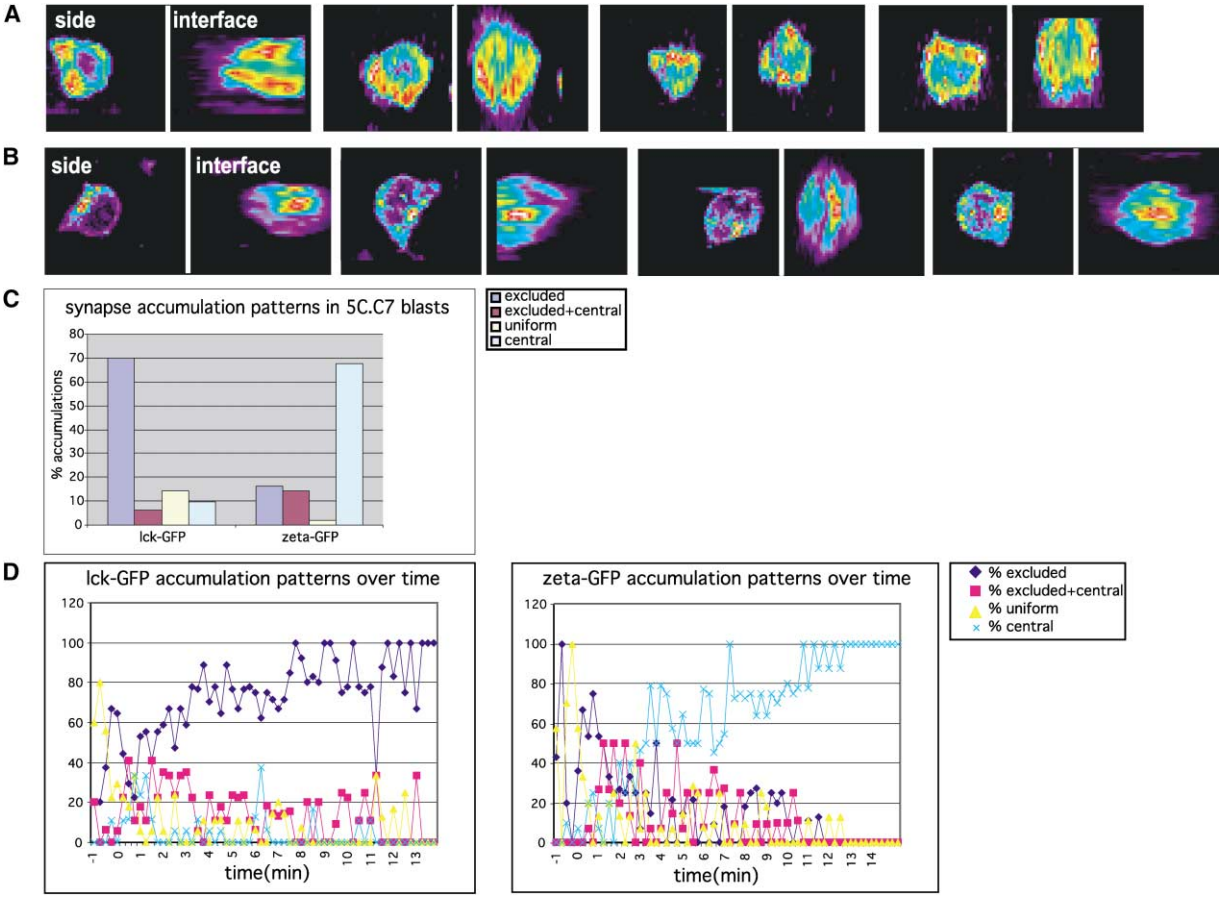

Figure 5. lck-GFP Is Progressively Recruited to the Periphery, while CD3ζ-GFP Is Recruited to the Center of the Synapse

Retrospective conjugates of lck-GFP (A) or CD3ζ-GFP (B) 5C.C7 blasts interacting with MCC-pulsed CH27 cells were generated and 3-D reconstructions of the GFP images were made. Z stacks were deconvolved using 60 iterations of a blind 3D algorithm (AutoQuant). Each pair of panels represents a side view of the conjugated cell on the left and an en face view of the immunological synapse on the right. (C) 111 CD3ζ-GFP and 83 lck-GFP 5C.C7 retrospective conjugates were scored for synapse accumulation patterns. (D) Seventeen lck-GFP and fifteen CD3ζ-GFP conjugates were scored for accumulation patterns over time. Around calcium flux, a large percentage of conjugates have both lck and CD3ζ at the synapse periphery. A diversity of patterns is observed as the synapse begins to mature. By 4 min after flux, lck-GFP is predominantly recruited to the synapse periphery, while CD3ζ-GFP is recruited to the center.

deconvolved images in Figure 7A show an intracellular pool of endogenous lck in both. We then stained lck-GFP-expressing D10 cells with an anti-β tubulin antibody. This shows that the intracellular lck pool tightly surrounds the microtubule organizing center (MTOC), as identified by the high-intensity region in the β tubulin stain (Figure 7B). This localization suggests that intracellular lck might be associated with microtubules. Indeed, the pool is dispersed into numerous small accumulations following treatment with nocodazole (Figure 7C). These data suggest that the intracellular pool translocates to the interface concomitantly with MTOC reorientation.

To narrow the identity of the intracellular pool with respect to cellular organelles, we stained lck-GFP D10 cells with anti-γ-adaptin to identify the trans-golgi network or with anti-transferrin receptor to stain recycling endosomes. In addition, TRITC-dextran uptake labels late endosomes. As seen in Figure 7D, neither γ-adaptin nor TRITC-dextran colocalize with the intracellular pool; however, anti-transferrin receptor colocalizes extensively. To confirm this result, a pulse-chase experiment was performed with labeled transferrin. Initially, transferrin is seen only on cell membranes (Figure 7E top row), but over time it is internalized so that by 20 min, it is largely colocalized with the intracellular pool, suggesting colocalization with recycling endosomes. The labeled T cells were then imaged during conjugate formation with CA-pulsed CH27 cells, demonstrating that transferrin and intracellular lck translocate to the interface simultaneously (Figure 7F and Supplemental Movie S9 at http://www.immunity.com/cgi/content/full/17/6/809/DC1).

Translocation of intracellular lck to the immunological synapse suggests that lck may contribute to T cell signaling in the late synapse. To address this possibility, we examined antigen-induced 5C.C7 T cell blast proliferation upon addition of PP2, a potent lck and fyn inhibitor (Hanke et al., 1996), at various time points after T cell:APC admixture. Proliferation is inhibited completely

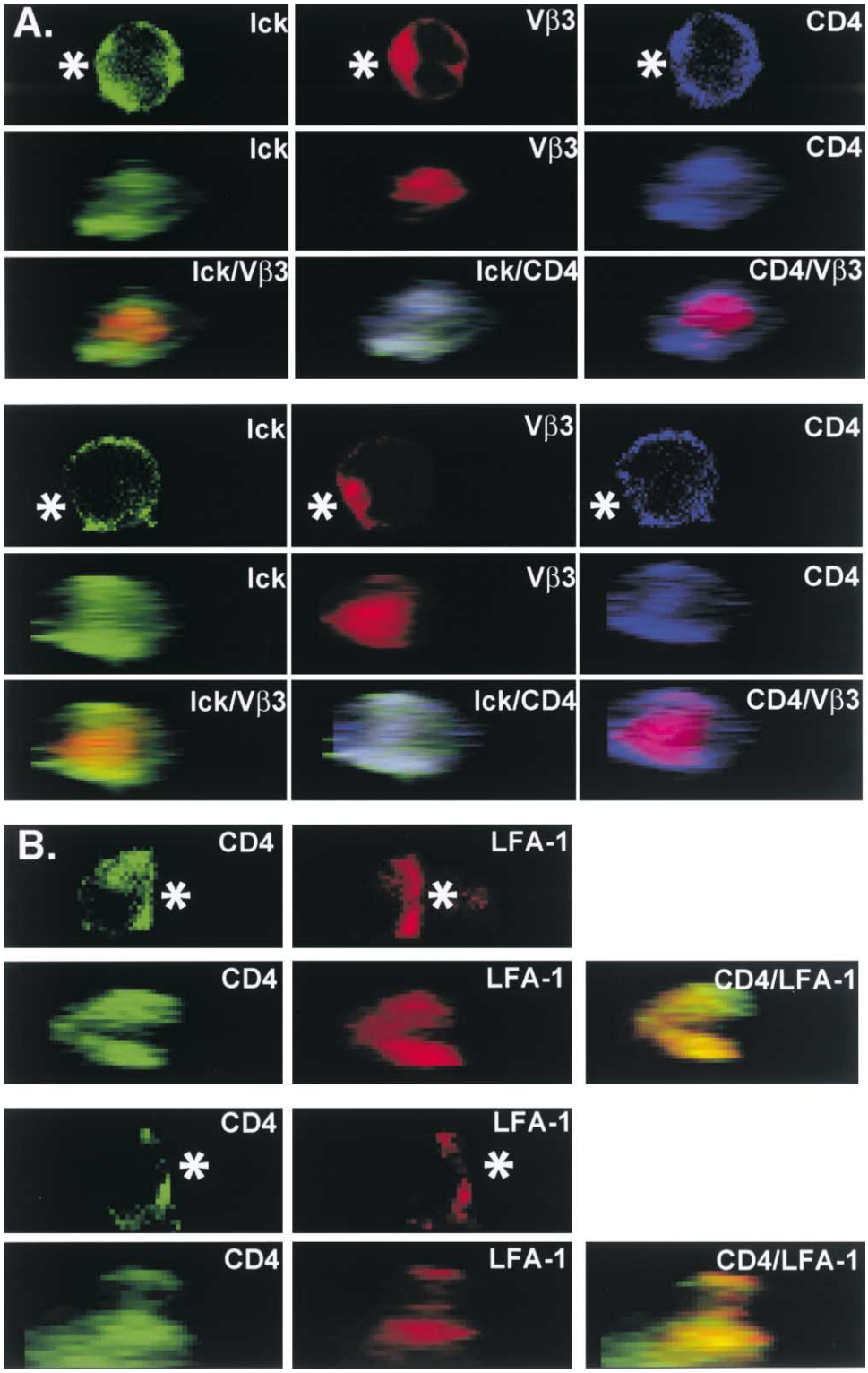

Figure 6. Endogenous Ick and CD4 Are Predominantly at the Periphery, while TCR Is in the Center of the Mature Immunological Synapse

5C.C7 blasts interacted with MCC-pulsed CH27 cells for 30 min. The conjugates were then fixed, permeabilized, and stained for endogenous (A) Ick, CD4, and Vβ3 or (B) CD4 and LFA-1. Z stacks of each fluorophore were acquired at 1 μm intervals and were used to generate 3-D reconstructions. The top panel of each conjugate represents single z slices through the center of the cell, and the asterisk indicates the location of the APC. The remaining panels represent an immunological synapse viewed en face as labeled. Note that Ick and CD4 largely colocalize at the periphery, leaving a region of lower intensity in the center of the synapse. TCR is predominantly found in the center of the synapse (c-SMAC), while LFA-1 and CD4 colocalize to the peripheral region (p-SMAC).

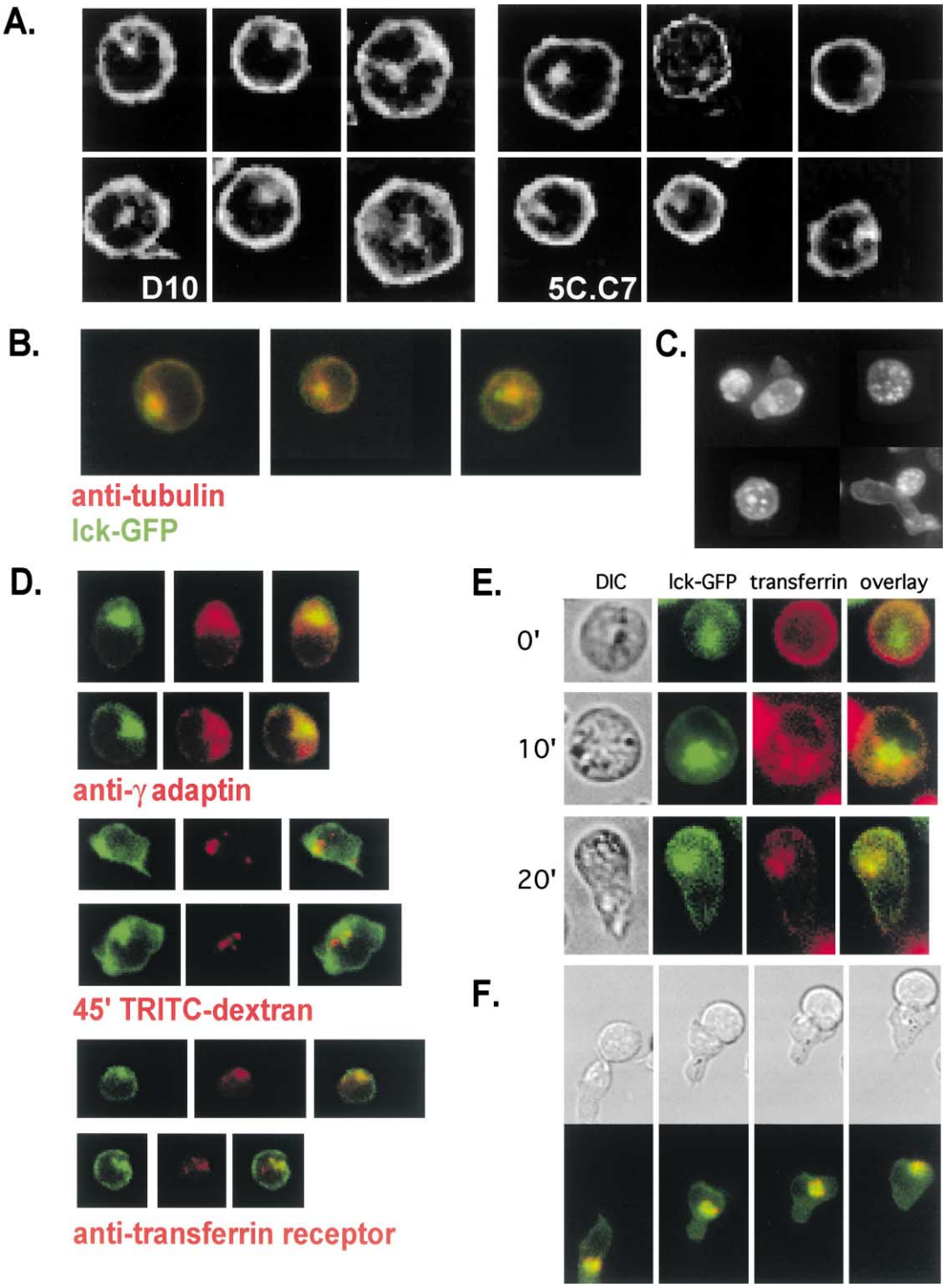

Figure 7. Endogenous lck Can Be Found in an Intracellular Pool in 5C.C7 Blasts and in D10 Cells, and This Pool Surrounds the MTOC and Colocalizes with Recycling Endosomes

(A) D10 cells and 5C.C7 blasts were fixed, permeabilized, and stained with an anti-lck antibody as in Figure 6. Images were captured at 1 μm intervals and were deconvolved using 2-D deconvolution with a nearest-neighbors algorithm. Each panel is a single slice through the middle of different cells, showing a clear intracellular pool of lck in both 5C.C7 and D10 cells.

(B) lck-GFP D10 cells were fixed, permeabilized, and stained for β-tubulin. The cells were then imaged as in (A) and a central region of three different cells is displayed, showing that the lck intracellular pool tightly surrounds the MTOC, which is seen as a bright red accumulation.

(C) lck-GFP D10 cells were treated with 100 μM nocodazole to disrupt the microtubule cytoskeleton and 3-D reconstructions of the GFP images were then made. Note that the intracellular pool is dispersed.

(D) lck-GFP D10 cells were fixed, permeabilized, and stained with anti-γ-adaptin or anti-transferrin receptor, or they were allowed to uptake

when PP2 is added within 1 hr of admixture, and is significantly reduced when PP2 is added after 24 hr (Supplemental Figure S4 at http://www.immunity.com/cgi/content/full/17/6/809/DC1). These data strongly indicate that lck and/or fyn tyrosine kinase activity is essential for T cell activation for well over an hour after conjugate formation.

Discussion

Using GFP fusions, we characterized the relative spatial and temporal recruitment of lck and CD3ζ to the immunological synapse. We find that both are rapidly recruited to the synapse where they are stably maintained for at least 15 min (Figures 3 and 4). Both lck and CD3ζ are initially recruited to the synapse periphery and then move dynamically throughout the synapse during the first few minutes after calcium flux. CD3ζ then becomes enriched in the center while lck is enriched at the synapse periphery (Figure 5). Endogenous lck and TCR exhibit the same distinct accumulation patterns (Figure 6). These data suggest a limited window of opportunity for lck and CD3ζ to interact efficiently at the nascent immunological synapse.

Our data also suggest that CD4 and lck remain associated throughout synapse formation. The disparate spatial accumulations of CD3ζ and lck mirror our previous studies of CD3ζ and CD4 segregation in a T cell line (Krummel et al., 2000) and are in contrast to studies of Zal and colleagues (2002) who found CD3ζ and CD4 dispersed throughout the synapse in a T cell hybridoma. Indeed, we find that lck colocalizes with CD4 at the mature immunological synapse periphery (Figure 6). Most importantly, anti-CD4 capping recruits most of the detectable membrane proximal lck (Supplemental Figure S1 at http://www.immunity.com/cgi/content/full/17/6/809/DC1), suggesting CD4 association of lck at the synapse.

Importantly, different CD3ζ and CD4/lck accumulation patterns do not reflect an absolute molecular segregation. Instead, we observe a change in the relative distribution of molecules, which could have a substantial impact on signals transduced via CD3 ITAM phosphorylation. If lck and CD3 cannot interact efficiently, many fewer second messengers would be generated, significantly impacting signals transduced through the TCR. This concept has been mathematically verified in the kinetic proofreading (McKeithan, 1995) and kinetic discrimination (Rabinowitz et al., 1996a) models in which changes in the kinetics of TCR-peptide:MHC binding alter the relative concentrations of signaling intermediates, such that early intermediates result in different signals than later intermediates. Thus, enrichment of lck and CD3ζ in different regions of the synapse could reduce the number of interactions of sufficient duration to result in complete ITAM phosphorylation, generating different or reduced signals. In support of this are data showing that even 2-fold changes in the number of genes encoding signaling molecules can have dramatic effects on lymphocyte activation (Cornall et al., 1998). Therefore, even a 2-fold decrease in association between lck and CD3ζ would alter TCR-mediated signals as the synapse matures, allowing the immunological synapse to generate varying signals throughout the duration of T cell activation.

It has been suggested that lck activity at the synapse is short lived and limited to the periphery (Holdorf et al., 2002; Lee et al., 2002). Consistent with these data, we find that lck is in close proximity to CD3ζ at the nascent synapse periphery, but over the next couple of minutes, lck and CD3ζ are found throughout the synapse, where they may have opportunities to interact. However, in contrast to the conclusion of Holdorf et al. that lck is released from CD4 and maintained in the c-SMAC, we find that lck accumulates peripherally with CD4 in mature T cell synapses (Figures 5 and 6). Furthermore, it has been demonstrated that autophosphorylation of tyrosine Y394 is induced following anti-CD4 co-capping, but not following anti-CD3 treatment or other stimuli that are known to induce T cell activation via lck (Luo and Sefton, 1990). Therefore, while anti-phopho-Y394 may recognize a particular form of activated lck, it does not detect all forms, so lck activity at the immunological synapse may be longer lived than previously suggested. Indeed, we find that blocking lck and/or fyn activity as late as 1 hr after T cell:APC admixture blocks T cell proliferation, consistent with the importance of lck activity at the synapse well beyond the onset of synapse formation (Supplemental Figure S4 at http://www.immunity.com/cgi/content/full/17/6/809/DC1). While PP2 blocks both lck and fyn, the effect that we see is more likely due to an lck blockade as analyses of knockout mice show that lck is more critical in peripheral T cell activation than fyn (Appleby et al., 1992; Molina et al., 1992; Stein et al., 1992). Thus, translocation of lck after synapse formation is likely to make an important contribution to T cell activation.

As lck is the first tyrosine kinase to initiate signaling downstream of an engaged TCR, and CD3ζ ITAM phosphorylation patterns have been shown to vary following APL stimulation (Kersh et al., 1998), we reasoned that lck recruitment might also vary. Indeed, we have recently reported an alteration in the relative localizations of lck and CD3ζ within thymocyte immunological synapses during negative selection, suggesting that alternate synapse architecture contributes to distinct TCR-mediated signals (Richie et al., 2002). However, in mature T cells, we did not find a difference in the extent, timing, or pattern of lck recruitment to the synapse following weak agonist signaling (Figure 3). Indeed, the only reproducible difference was a reduced efficiency of conjugate

TRITC-dextran before imaging. A single slice through the center of two different cells for each stain is shown. Note that transferrin receptor colocalizes with the intracellular pool of lck-GFP.

(E) lck-GFP D10 cells were pulse/chased for the indicated times with Texas Red-transferrin. A central slice for each cell is shown.

(F) Time points from conjugate formation of an lck-GFP D10 cell with internalized TR-transferrin. Note the simultaneous translocation of internal lck and transferrin to the interface. See Supplemental Movie S9 at http://www.immunity.com/cgi/content/full/17/6/809/DC1 for the complete timecourse.

formation (Figure 3D). Previous work has shown that weak agonists induce less T cell proliferation but similar acid release and calcium flux as strong agonists (Rabinowitz et al., 1996b). Our data are consistent with these observations: if a smaller percentage of T cells are induced to form conjugates by weak agonists, then the maximum proliferation of the population would be reduced.

In both the 5C.C7 and D10 systems, antagonists failed to induce significant calcium flux or lck accumulation at the synapse (Figure 3). Furthermore, they did not induce conjugate formation any more efficiently than unpulsed CH27 cells (data not shown and Figure 3D). These data are consistent with previous studies demonstrating that antagonists fail to induce acid release, calcium flux, or T cell proliferation above the level induced by endogenous APC peptides (Rabinowitz et al., 1996b; Wulfing et al., 1997). However, our data differ from the results of Huang et al. (2000) who find that antagonists induce efficient conjugate formation. This is likely to reflect differences in experimental design, as Huang et al. used a much higher concentration of antagonist peptides (55 μM versus 1 μM).

Unexpectedly, we observed translocation of intracellular lck to the synapse of both D10 and 5C.C7 cells (Supplemental Movies S1 and S5 at http://www.immunity.com/cgi/content/full/17/6/809/DC1). Staining for endogenous lck revealed that this pool was not a product of lck-GFP mislocalization (Figure 7A). A similar intracellular pool has been described in Jurkat cells (Ley et al., 1994), and lck has been biochemically identified in endosomes of nonactivated T cells (Luton et al., 1997). As in Jurkat cells, intracellular lck surrounds the MTOC in D10 cells and can be dispersed by the microtubule dissociating agent nocodazole (Figures 7B and 7C). Consistent with localization to recycling endosomes, intracellular lck is colocalized with transferrin receptor and internalized transferrin (Figures 7D, 7E, and 7F). Thus, intracellular lck might recycle back to the membrane, providing an additional source of the kinase at mature synapses. Indeed, both labeled transferrin and the intracellular lck pool translocate to the T cell:APC interface following agonist stimulation (Figure 7F and Supplemental Movie S9 at http://www.immunity.com/cgi/content/full/17/6/809/DC1). Kuhn and colleagues (2002) have recently demonstrated that the MTOC reorients such that it is located at the periphery of the synapse, consistent with localization of lck at the synapse periphery in retrospective conjugates (Figure 5A). There is precedence for the fusion of an intracellular pool of signaling molecules with the plasma membrane, as CTLA-4 has recently been shown to act in a comparable manner (Egen and Allison, 2002). It is known that a T cell must interact with an APC for at least 2 hr to commit to activation (Karttunen and Shastri, 1991; Lee et al., 2002). Possibly, intracellular lck provides a bolus of kinase activity needed for full activation of the T cell. Interestingly, this translocation of intracellular lck may place it in proximity to CD45 molecules that are on intracellular membranes proximal to the synapse (Johnson et al., 2000), potentially leading to lck activation at this location. Alternatively, lck could play a regulatory role in T cell signaling along with CTLA-4 (Egen and Allison, 2002). It is also possible that intracellular lck could counter the activity of CTLA-4-associated phosphatases. Future studies are needed to address these possibilities.

Our data on lck recruitment to the immunological synapse, along with a wealth of previous experimentation, suggests a multistage role for lck in T cell activation. First, lck initiates signaling by phosphorylating CD3 ITAMS following the engagement of a sufficient but small number of TCRs (Iwashima et al., 1994). Rapid reorganization of the actin cytoskeleton follows (Dustin and Cooper, 2000), recruiting molecules such as CD3, CD4, CD28, CD45, and lck to the immunological synapse (Bromley et al., 2001; Johnson et al., 2000; Krummel et al., 2000). At this point, lck may play a second signaling role by contributing to CD3 ITAM phosphorylations in nascent synapses, where we find that lck and CD3ζ are colocalized first at the synapse periphery and then throughout the synapse (Figure 3). This second wave of lck activity may strengthen TCR-mediated signals and/or establish cellular polarity (Davis and van der Merwe, 2001). In addition, lck may play a role in integrin affinity maturation, allowing for conjugate stabilization. It has been shown that src-family kinases can contribute to integrin signaling (Cary et al., 2002), and T cell:B cell conjugation is dependent on lck, but not ZAP-70, implying a distinct role for lck in conjugate stabilization (Morgan et al., 2001). Once molecules have spatially segregated within the mature synapse, the MTOC is recruited to the T cell:B cell interface (Kuhn and Poenie, 2002; Kupfer et al., 1987; Lowin-Kropf et al., 1998). Interestingly, we find that a bolus of intracellular lck translocates to the synapse, concomitant with MTOC reorientation (Supplemental Figure S2, Figure 7, and Supplemental Movie S9 at http://www.immunity.com/cgi/content/full/17/6/809/DC1). Thus, lck may play a third role in T cell signaling by contributing to signals emanating from late mature synapses. Indeed, Supplemental Figure S4 (http://www.immunity.com/cgi/content/full/17/6/809/DC1) demonstrates that lck and/or fyn activity is essential for T cell activation for at least 1 hr after T cell:APC admixture, suggesting that lck contributes to T cell activation following synapse formation.

Experimental Procedures

Constructs and Generation of Cell Lines and Blasts

cDNAs for CD3ζ and lck were cloned into EGFP-N1 (Clontech) to generate in frame carboxy terminal EGFP fusion constructs (Krummel et al., 2000). JCAM1.6 cells were transfected by electroporation using standard protocols. Transfectants were selected in G418 (Sigma) and screened for GFP expression. cDNAs for lck-GFP and CD3ζ-GFP were subcloned into the retroviral vector pIB (gift from Cenk Sumen) and were transfected into Phoenix-ecotropic producer cells (gift of Dr. Garry Nolan), which were stably selected and maintained in 10 μg/ml blasticidin (Invitrogen). The producer lines were monitored for GFP expression. Virus was collected and concentrated as previously described (Richie et al., 2002).

5C.C7 blasts were transduced with retrovirus and utilized for conjugate formation as previously described (Richie et al., 2002). D10 cells were maintained by stimulation of 10^6 cells with 10^7 fresh, irradiated B10.BR splenocytes pulsed with 100 μg/ml whole conalbumin (Sigma) every 7 days in 10 ml complete RPMI containing 10% FBS, 100 U/ml penicillin/streptomycin, 2 mM L-glutamine, and 50 μM β-mercaptoethanol. 24 hr poststimulation one flask of D10 cells was spin infected in a 24-well plate in 1 ml concentrated retrovirus (Richie et al., 2002). 24 hr later, the cells were transferred to 5 ml

of complete RPMI + 2% IL-2 + 20 μg/ml blasticidin. GFP+ cells were sorted by FACS and maintained as for nontransduced cells with the addition of 10 μg/ml blasticidin. Both GFP+ 5C.C7 blasts and D10 cells were monitored by FACS for normal expression of TCR, CD4, and CD28.

Calcium Flux Analysis

Jurkat, JCAM1.6, and reconstituted JCAM1.6 lines were loaded with 1 μM indo-1, AM (Molecular Probes) according to manufacturer's instructions. Propidium iodide was used to exclude dead cells. Live cells were analyzed at 37°C on a modified FACStar (FACS facility, Stanford University) with a clock that recorded elapsed time. The ratio of 405/485 emission, an indicator of intracellular calcium concentration, was monitored following addition of a saturating amount of monoclonal antibody C305 and then 1 μM ionomycin (Sigma).

Proliferation Assays

10^4 D10 cells or 5C.C7 blasts that had been rested for 5 days were incubated with 5×10^4 irradiated B10.BR splenocytes/well in 100 μl in a 96-well plate. 0-100 μg/ml whole conalbumin were added to triplicate wells of D10 cells, and 5 μM MCC was added to the indicated wells of 5C.C7 blasts. PP2 was added to the blasts at the indicated times after T cell:splenocyte admixture. 72 hr later for D10 and 48 hr later for 5C.C7 blasts 1 μCi ^{3}H-Thymidine was added/well. After 16 hr, the plates were harvested, and the filter paper was analyzed by liquid scintillation. Counts from triplicate wells were averaged.

Imaging

Transduced D10 or 5C.C7 conjugates were loaded with 1 μM fura-2, AM (Molecular Probes) for 20 min prior to imaging. The cells were washed and 2×10^5 cells were put into an 8-well glass-bottom chamber slide (Labtek/Nunc). 10^5 peptide-pulsed CH27 B cells were allowed to settle onto the slide at the onset of imaging.

Imaging was carried out on a previously described microscope system (Richie et al., 2002). For timelapse experiments, images were taken every 15 s for 15 min. Microscope control, data acquisition, and image analysis were performed in Metamorph (Universal Imaging). In time-lapse experiments, bleaching was corrected using a previously described algorithm (Krummel et al., 2000).

Co-Capping, Blocking, and Cytoskeletal Inhibitor Experiments

For co-capping, lck-GFP D10 cells were incubated on ice for 20 min with biotinylated primary antibodies against CD4 (GK1.5), CD28 (37.51), or CD3 (145-2C11) (Pharmingen) followed by Av-PE (Pharmingen) at 37°C for 20 min. The cells were fixed in 2% paraformaldehyde, mounted on slides, and imaged. To disrupt the actin or microtubule cytoskeleton, T cells were incubated with 100 μM colchicine (Sigma) or 100 μM nocodazole (Sigma) for 30 min prior to imaging.

Immunofluorescence and Transferrin or Dextran Uptake

5C.C7 blasts were allowed to conjugate for 30 min with MCC-pulsed CH27 B cells on poly-L-lysine coated slides (Wescor). The cells were fixed in 4% paraformaldehyde for 10 min and blocked in PBS containing 1% FBS + .3% saponin for 1 hr at room temperature. The following primary antibodies were added to the slides for 1 hr in the dark: monoclonal anti-lck clone 3A5 (Santa Cruz Biotechnology), APC-conjugated anti-CD4 clone GK1.5 (Pharmingen), and PE-conjugated anti-Vβ3 clone KJ25 (Pharmingen). The secondary Cy-3 conjugated anti-mouse Ig, Fcγ fragment-specific antibody (Jackson ImmunoResearch) was added for 1 hr in the dark. The slides were mounted in ProLong Antifade (Molecular Probes).

For staining of intracellular organelles, lck-GFP D10 cells were fixed, permeabilized in 1% Triton x-100, and stained with primary antibodies against γ-adaptin (AP1m, Pharmingen), human transferrin receptor (Enns et al., 1981), or β-tubulin (Sigma) followed by PE-conjugated anti-mouse, rhodamine-conjugated anti-goat, or rhodamine-conjugated anti-mouse antibodies, respectively. For dextran uptake, lck-GFP D10 cells were resuspended in 5 mg/ml TRITC-dextran (Sigma) and incubated at 37°C for 45 min.

For the transferrin pulse-chase, lck-GFP D10 cells were chilled on ice and incubated with 10 μg/ml Texas Red-conjugated transferrin (Molecular probes) for 30 min. The cells were washed twice and incubated at 37°C for the indicated periods of time prior to imaging. After 20 min, CA-pulsed CH27 cells were added and timelapse images were obtained every 15 s for 15 min.

Acknowledgments

We thank Cenk Sumen for the pIB construct and Björn Lillemeier for assistance. L.I.R.E. and P.J.R.E are Howard Hughes Medical Institute Predoctoral Fellows. M.M.D. is a Howard Hughes Investigator. Supported by grants from the National Institutes of Health and the Howard Hughes Medical Institute (to M.M.D).

Received: May 31, 2002
Revised: September 30, 2002

References

Abraham, N., Miceli, M.C., Parnes, J.R., and Veillette, A. (1991). Enhancement of T-cell responsiveness by the lymphocyte-specific tyrosine protein kinase p56lck. Nature *350*, 62–66.

Anderson, P., Blue, M.L., Morimoto, C., and Schlossman, S.F. (1987). Cross-linking of T3 (CD3) with T4 (CD4) enhances the proliferation of resting T lymphocytes. J. Immunol. *139*, 678–682.

Appleby, M.W., Gross, J.A., Cooke, M.P., Levin, S.D., Qian, X., and Perlmutter, R.M. (1992). Defective T cell receptor signaling in mice lacking the thymic isoform of p59fyn. Cell *70*, 751–763.

Bromley, S.K., Iaboni, A., Davis, S.J., Whitty, A., Green, J.M., Shaw, A.S., Weiss, A., and Dustin, M.L. (2001). The immunological synapse and CD28-CD80 interactions. Nat. Immunol. *2*, 1159–1166.

Cary, L.A., Klinghoffer, R.A., Sachsenmaier, C., and Cooper, J.A. (2002). SRC catalytic but not scaffolding function is needed for integrin-regulated tyrosine phosphorylation, cell migration, and cell spreading. Mol. Cell. Biol. *22*, 2427–2440.

Cornall, R.J., Cyster, J.G., Hibbs, M.L., Dunn, A.R., Otipoby, K.L., Clark, E.A., and Goodnow, C.C. (1998). Polygenic autoimmune traits: Lyn, CD22, and SHP-1 are limiting elements of a biochemical pathway regulating BCR signaling and selection. Immunity *8*, 497–508.

Davis, S.J., and van der Merwe, P.A. (2001). The immunological synapse: required for T cell receptor signalling or directing T cell effector function? Curr. Biol. *11*, R289–291.

Dittel, B.N., Sant'Angelo, D.B., and Janeway, C.A., Jr. (1997). Peptide antagonists inhibit proliferation and the production of IL-4 and/or IFN-gamma in T helper *1*, T helper *2*, and T helper 0 clones bearing the same TCR. J. Immunol. *158*, 4065–4073.

Dustin, M.L., and Cooper, J.A. (2000). The immunological synapse and the actin cytoskeleton: molecular hardware for T cell signaling. Nat. Immunol. *1*, 23–29.

Dustin, M.L., Olszowy, M.W., Holdorf, A.D., Li, J., Bromley, S., Desai, N., Widder, P., Rosenberger, F., van der Merwe, P.A., Allen, P.M., et al. (1998). A novel adaptor protein orchestrates receptor patterning and cytoskeletal polarity in T-cell contacts. Cell *94*, 667–677.

Egen, J.G., and Allison, J.P. (2002). Cytotoxic T lymphocyte antigen-4 accumulation in the immunological synapse is regulated by TCR signal strength. Immunity *16*, 23–35.

Enns, C.A., Shindelman, J.E., Tonik, S.E., and Sussman, H.H. (1981). Radioimmunochemical measurement of the transferrin receptor in human trophoblast and reticulocyte membranes with a specific anti-receptor antibody. Proc. Natl. Acad. Sci. USA *78*, 4222–4225.

Fazekas de St. Groth, B., Patten, P.A., Ho, W.Y., Rock, E.P., and Davis, M.M. (1993). An analysis of T cell receptor-ligand interaction using a transgenic antigen model for T cell tolerance and T cell receptor mutagenesis. In Molecular Mechanisms of Immunological Self-Recognition, F.W. Alt and H.J. Vogel, eds. (San Diego: Academic Press), pp. 123–127.

Glaichenhaus, N., Shastri, N., Littman, D.R., and Turner, J.M. (1991). Requirement for association of p56lck with CD4 in antigen-specific signal transduction in T cells. Cell *64*, 511–520.

Grakoui, A., Bromley, S.K., Sumen, C., Davis, M.M., Shaw, A.S., Allen, P.M., and Dustin, M.L. (1999). The immunological synapse: a

molecular machine controlling T cell activation. Science *285*, 221–227.

Hanke, J.H., Gardner, J.P., Dow, R.L., Changelian, P.S., Brissette, W.H., Weringer, E.J., Pollok, B.A., and Connelly, P.A. (1996). Discovery of a novel, potent, and Src family-selective tyrosine kinase inhibitor. J. Biol. Chem. *271*, 695–701.

Holdorf, A.D., Green, J.M., Levin, S.D., Denny, M.F., Straus, D.B., Link, V., Changelian, P.S., Allen, P.M., and Shaw, A.S. (1999). Proline residues in CD28 and the Src homology (SH)3 domain of Lck are required for T cell costimulation. J. Exp. Med. *190*, 375–384.

Holdorf, A.D., Lee, K.H., Burack, W.R., Allen, P.M., and Shaw, A.S. (2002). Regulation of Lck activity by CD4 and CD28 in the immunological synapse. Nat. Immunol. *3*, 259–264.

Huang, J., Sugie, K., La Face, D.M., Altman, A., and Grey, H.M. (2000). TCR antagonist peptides induce formation of APC-T cell conjugates and activate a Rac signaling pathway. Eur. J. Immunol. *30*, 50–58.

Iwashima, M., Irving, B.A., van Oers, N.S., Chan, A.C., and Weiss, A. (1994). Sequential interactions of the TCR with two distinct cytoplasmic tyrosine kinases. Science *263*, 1136–1139.

Johnson, K.G., Bromley, S.K., Dustin, M.L., and Thomas, M.L. (2000). A supramolecular basis for CD45 tyrosine phosphatase regulation in sustained T cell activation. Proc. Natl. Acad. Sci. USA *97*, 10138–10143.

Kane, L.P., Lin, J., and Weiss, A. (2000). Signal transduction by the TCR for antigen. Curr. Opin. Immunol. *12*, 242–249.

Karttunen, J., and Shastri, N. (1991). Measurement of ligand-induced activation in single viable T cells using the lacZ reporter gene. Proc. Natl. Acad. Sci. USA *88*, 3972–3976.

Kaye, J., Porcelli, S., Tite, J., Jones, B., and Janeway, C.A., Jr. (1983). Both a monoclonal antibody and antisera specific for determinants unique to individual cloned helper T cell lines can substitute for antigen and antigen-presenting cells in the activation of T cells. J. Exp. Med. *158*, 836–856.

Kersh, E.N., Shaw, A.S., and Allen, P.M. (1998). Fidelity of T cell activation through multistep T cell receptor zeta phosphorylation. Science *281*, 572–575.

Krummel, M.F., Sjaastad, M.D., Wulfing, C., and Davis, M.M. (2000). Differential clustering of CD4 and CD3zeta during T cell recognition. Science *289*, 1349–1352.

Kuhn, J.R., and Poenie, M. (2002). Dynamic polarization of the microtubule cytoskeleton during CTL-mediated killing. Immunity *16*, 111–121.

Kupfer, A., Swain, S.L., and Singer, S.J. (1987). The specific direct interaction of helper T cells and antigen-presenting B cells. II. Reorientation of the microtubule organizing center and reorganization of the membrane-associated cytoskeleton inside the bound helper T cells. J. Exp. Med. *165*, 1565–1580.

Lee, K.H., Holdorf, A.D., Dustin, M.L., Chan, A.C., Allen, P.M., and Shaw, A.S. (2002). T cell receptor signaling precedes immunological synapse formation. Science *295*, 1539–1542.

Lewis, L.A., Chung, C.D., Chen, J., Parnes, J.R., Moran, M., Patel, V.P., and Miceli, M.C. (1997). The Lck SH2 phosphotyrosine binding site is critical for efficient TCR-induced processive tyrosine phosphorylation of the zeta-chain and IL-2 production. J. Immunol. *159*, 2292–2300.

Ley, S.C., Marsh, M., Bebbington, C.R., Proudfoot, K., and Jordan, P. (1994). Distinct intracellular localization of Lck and Fyn protein tyrosin kinases in human T lymphocytes. J. Cell Biol. *125*, 639–649.

Lowin-Kropf, B., Shapiro, V.S., and Weiss, A. (1998). Cytoskeletal polarization of T cells is regulated by an immunoreceptor tyrosine-based activation motif-dependent mechanism. J. Cell Biol. *140*, 861–871.

Luo, K.X., and Sefton, B.M. (1990). Cross-linking of T-cell surface molecules CD4 and CD8 stimulates phosphorylation of the lck tyrosine protein kinase at the autophosphorylation site. Mol. Cell. Biol. *10*, 5305–5313.

Luton, F., Legendre, V., Gorvel, J.P., Schmitt-Verhulst, A.M., and Boyer, C. (1997). Tyrosine and serine protein kinase activities associated with ligand-induced internalized TCR/CD3 complexes. J. Immunol. *158*, 3140–3147.

McKeithan, T.W. (1995). Kinetic proofreading in T-cell receptor signal transduction. Proc. Natl. Acad. Sci. USA *92*, 5042–5046.

Molina, T.J., Kishihara, K., Siderovski, D.P., van Ewijk, W., Narendran, A., Timms, E., Wakeham, A., Paige, C.J., Harmann, K.-U., Veillette, A., et al. (1992). Profound block in thymocyte development in mice lacking p56lck. Nature *357*, 161–164.

Monks, C.R., Freiberg, B.A., Kupfer, H., Sciaky, N., and Kupfer, A. (1998). Three-dimensional segregation of supramolecular activation clusters in T cells. Nature *395*, 82–86.

Morgan, M.M., Labno, C.M., Van Seventer, G.A., Denny, M.F., Straus, D.B., and Burkhardt, J.K. (2001). Superantigen-induced T cell:B cell conjugation is mediated by LFA-1 and requires signaling through Lck, but not ZAP-70. J. Immunol. *167*, 5708–5718.

Rabinowitz, J.D., Beeson, C., Lyons, D.S., Davis, M.M., and McConnell, H.M. (1996a). Kinetic discrimination in T-cell activation. Proc. Natl. Acad. Sci. USA *93*, 1401–1405.

Rabinowitz, J.D., Beeson, C., Wulfing, C., Tate, K., Allen, P.M., Davis, M.M., and McConnell, H.M. (1996b). Altered T cell receptor ligands trigger a subset of early T cell signals. Immunity *5*, 125–135.

Richie, L.I., Ebert, P.J.R., Wu, L.C., Krummel, M.F., Owen, J.J.T., and Davis, M.M. (2002). Imaging synapse formation during thymocyte selection: inability of CD3zeta to form a stable central accumulation during negative selection. Immunity *16*, 595–606.

Rudd, C.E., Barber, E.K., Burgess, K.E., Hahn, J.Y., Odysseos, A.D., Sy, M.S., and Schlossman, S.F. (1991). Molecular analysis of the interaction of p56lck with the CD4 and CD8 antigens. Adv. Exp. Med. Biol. *292*, 85–96.

Stein, P.L., Lee, H.M., Rich, S., and Soriano, P. (1992). pp59fyn mutant mice display differential signaling in thymocytes and peripheral T cells. Cell *70*, 741–750.

Straus, D.B., and Weiss, A. (1992). Genetic evidence for the involvement of the lck tyrosine kinase in signal transduction through the T cell antigen receptor. Cell *70*, 585–593.

Straus, D.B., Chan, A.C., Patai, B., and Weiss, A. (1996). SH2 domain function is essential for the role of the lck tyrosine kinase in T cell receptor signal transduction. J. Biol. Chem. *271*, 9976–9981.

Trowbridge, I.S., and Thomas, M.L. (1994). CD45: an emerging role as a protein tyrosine phosphatase required for lymphocyte activation and development. Annu. Rev. Immunol. *12*, 85–116.

Turner, J.M., Brodsky, M.H., Irving, B.A., Levin, S.D., Perlmutter, R.M., and Littman, D.R. (1990). Interaction of the unique N-terminal region of tyrosine kinase p56lck with cytoplasmic domains of CD4 and CD8 is mediated by cysteine motifs. Cell *60*, 755–765.

Wange, R.L., and Samelson, L.E. (1996). Complex complexes: signaling at the TCR. Immunity *5*, 197–205.

Wulfing, C., Rabinowitz, J.D., Beeson, C., Sjaastad, M.D., McConnell, H.M., and Davis, M.M. (1997). Kinetics and extent of T cell activation as measured with the calcium signal. J. Exp. Med. *185*, 1815–1825.

Zal, T., Zal, M.A., and Gascoigne, N.R. (2002). Inhibition of T cell receptor-coreceptor interactions by antagonist ligands visualized by live FRET imaging of T-hybridoma immunological synapse. Immunity *16*, 521–534.